ARMA 16-0085

SAND2016-1400C

Laboratory Scale Hydraulic Fracture of Marcellus Shale

Ingraham, M.D., D. Bolintineau, R.R. Rao, S.J. Bauer, E.C. Quintana, J.B. Lechman

Sandia National Laboratories, Albuquerque, NM, USA

Copyright 2016 ARMA, American Rock Mechanics Association

This paper was prepared for presentation at the 50th US Rock Mechanics / Geomechanics Symposium held in Houston, Texas, USA, 26-29 June 2016. This paper was selected for presentation at the symposium by an ARMA Technical Program Committee based on a technical and critical review of the paper by a minimum of two technical reviewers. The material, as presented, does not necessarily reflect any position of ARMA, its officers, or members. Electronic reproduction, distribution, or storage of any part of this paper for commercial purposes without the written consent of ARMA is prohibited. Permission to reproduce in print is restricted to an abstract of not more than 200 words; illustrations may not be copied. The abstract must contain conspicuous acknowledgement of where and by whom the paper was presented.

ABSTRACT: Performing experiments in the laboratory that mimic conditions in the field is challenging. In an attempt to understand hydraulic fracture in the field, an effort to duplicate the typical fracture pattern for long horizontal wells has been made. The typical "disks on a string" fracture formation is caused by properly orienting the long horizontal well such that it is parallel to the minimum principal stress direction, then fracturing the rock. In order to replicate this feature in the laboratory with a traditional cylindrical specimen the test must be performed under extensile stress conditions and the specimen must have been cored parallel to bedding in order to avoid failure along a bedding plane, and replicate bedding orientation in the field. Testing has shown that it is possible to form failure features of this type in the laboratory. A novel method for jacketing is employed to allow fluid to flow out of the fracture and leave the specimen without risking the integrity of the jacket; this allows proppant to be injected into the fracture, simulating loss of fracturing fluids to the formation, and allowing a solid proppant pack to be developed.

1. INTRODUCTION

The decrease in the price of oil increases the need for more efficient extraction of oil and gas from source rocks exploited by hydraulic fracturing. With the decline in oil and gas prices comes the need for more efficient and effective extraction from these reservoirs to maintain economic viability. This means that research into efficient extraction of oil and gas is more important than ever.

To this end, Sandia has endeavored to replicate aspects of in situ hydrofracturing in the lab, and prop said fractures. Proppant location data is coupled with the injection parameters and fluid rheology. This data is then used to inform flow simulations, which will then be used to understand relationships between injection parameters, proppant placement and fracture conductivity; thereby more effectively predicting proppant location in a fracture. This paper focuses on the methodology for generating and propping properly oriented fractures which are clearly visible using micro computed tomography (μCT). The modeling efforts will be presented separately in a future publication.

2. BACKGROUND

Generation of hydraulic fractures is not a new concept; the mechanics of hydraulic fracturing were described by Hubbert and Willis in 1957. Hydraulic fracturing has been used in determining in-situ stress conditions from borehole fracturing since the 1960s (ex. Kehle 1964, Haimson and Fairhurst 1969). Laboratory scale hydraulic fracture experiments have been taking place since the 1960s or earlier (ex. Pegler 1967, Zoback et al. 1977, Warpinski et al. 1982). These early studies focused on measuring the minimum principal stress magnitude and direction in the earth using hydraulic fracturing (ex. Kehle 1964, Haimson and Fairhurst 1969). Subsequently the interest shifted to transmission of fluids in the subsurface, and the interaction of hydraulic and natural fractures (ex. Zoback et al. 1977). Since then the focus has been on interaction with natural fractures, generation of fluid flow paths, and recently propping of hydraulic fractures (Wen et al. 2006, Fredd et al. 2000, Alramahi and Sundberg 2012). However, recent work has moved away from laboratory testing under in situ conditions towards validation of numerical simulations, which have so far focused on simplified geometry like flow between parallel plates (e.g. Morris and Chugunov, 2014, Lane and Thompson, 2010). This is because it has been shown that fractures can be generated, and proppant can be pumped into the fracture, but fracture geometry is usually simplified.

To this end, we have endeavored to hydraulically fracture real rock in the lab, and prop the fractures under conditions that most closely resemeble those found in the field, including bedding orientation. We have performed tests where the minimum principal stress is parallel to the borehole, i.e. under extensile conditions (ex. Sitchler et al. 2013), in order to generate fracture planes oriented normal to the borehole, and bedding, replicating the "disks on a string" configuration common in non-traditional shale gas reservoirs. These tests, coupled with CT scans, can then be mined for fracture geometry and proppant pack locations. Flow models can

be implemented that more closely capture the placement of proppant particles and fracture geometries. This enables a detailed investigation of fracture conductivities in real fracture geometries.

Ultimately the goal of this work is to improve modeling capability for the prediction of proppant packing in hydraulic fractures. Since proppant selection injection strategies are some of the few factors that can be controlled in a hydraulic fracture operation, optimization of those parameters is paramount in improving production from fractured wells.

3. MATERIALS AND METHODS

3.1. Westerly Granite

The goal of this work was to create laboratory hydraulic fractures in shale, however, due to the difficulty in obtaining specimens of sufficient size and quality to perform this type of test, a series of preliminary tests were performed on Westerly granite (UCS=197 MPa, Heap and Faulkner (2008)). The Westerly granite is a fine grained granodiorite; samples were taken from an oriented block from the quarried material used by (Krech et al. 1974) to describe this member of the standard rock suite for rapid excavation. The granodiorite has massive, fine-grained and equi-granular texture and has a modal analysis of plagioclase (43.0 %), microcline (22.0 %), quartz (24.6%), biotite (6.9%), muscovite (2.0%), zircon (1.0 %), and magnetite (0.9%). A reason for choosing Westerly granite is because it has been used for numerous studies in experimental rock deformation, and is generally considered homogeneous and isotropic with a 10% velocity anisotropy.

Westerly granite specimens measured 10.16 cm in diameter and 20.32 cm in length. Specimens were end ground to ensure parallelism per ASTM D4543 (1995). The specimen then had a 6.35 mm hole drilled in the middle of the specimen to a depth of approximately 10 cm., into which a piece of 6.35mm pipe with an internal diameter of 3.17 mm was epoxied to act as a casing. The pipe was placed such that the bottom 1.9 cm of the hole was left open. This pipe extended 1.9 cm beyond the top of the specimen to interface with and seal to the end cap so that fluid could be injected into the pipe at pressure, see Fig.1.

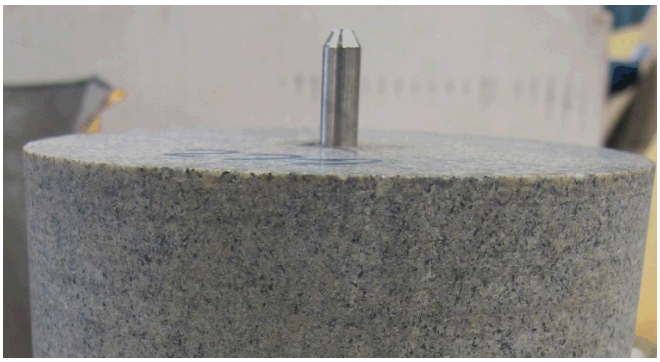

Fig. 1. Image of the casing pipe epoxied into place in the center of a specimen. The pipe extends beyond the top of the specimen in order to seal with the endcap, and the bottom 1.9 cm of the hole was left uncased.

The specimen was then wrapped in a stainless steel Feltmetal™ with another piece of the material placed on the bottom of the specimen. This was done to act as a path for the injected fluids to follow after traveling through the fracture, while not interfering with transferring load to the sample. This simultaneously lowered the possibility of a jacket rupture from high pressure injection fluids. This flow path was open to atmosphere on the bottom of the specimen. Fig. 2 shows the specimen wrapped in the frit material. End caps were then applied to the specimen and the specimen was jacketed in viton. The jacket was sealed with an o-ring and tie wires at each end cap.

Tests began by placing the specimen in a pressure vessel and hydrostatically loading to 10.3 MPa. An axial load of 3.3 MPa over confining pressure was applied to the specimen placing it into an axisymmetric compression stress state. Pore pressure was then elevated to the maximum capacity of the pump (25.9 MPa). Water was used for the fracturing fluid. For the granite specimens this was insufficient to induce fracture so the pore pressure was lowered and confinement was lowered to 6.9 MPa (axial stress was still 3.3 MPa over confining pressure). The pore system was repressurized to 25.9 and fracture induced.

After the rock is fractured with water, the fracture was determined to be open when water was flowing out the

Fig. 2. Specimen with end caps and wrapped in the steel frit material. The orange electrical tape is used to close the frit around the specimen and to connect the specimen, end cap and

frit together. This whole assembly is then jacketed in viton in the case of the granite or polyolefin in the case of the shale.

vent port connected to the bottom of the specimen, the fluid in the pump was changed to a guar based fluid which was laced with aluminum oxide particles with an average size of 104 microns. Aluminum oxide was chosen as a proppant material because of its high contrast when viewed in the μCT scanner when compared with silicate rocks, and because it was available in a size that would flow into the small fractures aperture well.

In subsequent testing, the aluminum oxide was replaced with silicon carbide. This was done because the fracturing fluid was guar and boric acid based, which the aluminum oxide reacted with, and significantly changed the rheology of the fracturing fluid.

3.2. Marcellus Shale

The Marcellus shale has an unconfined compressive strength of ~34-70MPa (Brown and Meckfessel, 2010), significantly lower than the granite. The minerology is highly dependent on the lithofacies but the content is typically 1-11% total organic, 30-50% clay, 5-35% carbonate and 35-60% quartz for not carbonate facies (Wang and Carr, 2012). The low strength has the potential to affect the fracturing process because the shale is weaker, meaning that it is possible to induce accidental fractures purely from loading. The cores, taken parallel to bedding, were 7.62 cm in diameter and approximately 15.2 cm in height, ASTM D4543 was followed in the preparation of the sample prior to the hole being drilled in the center of the specimen. Smaller specimens were necessary because of the size of the parent shale block. The hole was drilled to a depth of 7.6 cm, and then a piece of 6.35mm pipe with an internal diameter of 3.17 mm was epoxied into the hole. The pipe was placed such that the bottom 1.9 cm of the hole was left open. This pipe extended beyond the top of the specimen 1.9 cm to interface and sealed to the end cap

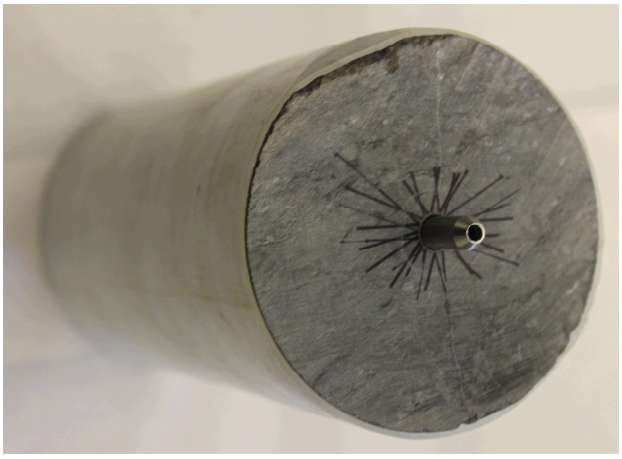

Fig. 3. Image of the top of a shale sample.

so that fluid could be injected into the pipe at high pressure, see Fig.3.

The specimen was wrapped in the stainless steel frit in the same manner as the granite samples. However the jacket for the shale was heat-shrink polyolefin secured with tie wires. As insurance against leaks, the ends of the polyolefin jacket were sealed to the endcaps with UV cure polyurethane.

Jacketed specimens were placed into a pressure vessel and the ends of the specimen were sealed to the bottom of the vessel and the vessel piston to allow for loading in an extensile stress state. The vessel was placed into a loading frame which controlled confining pressure and axial load/displacement and loaded hydrostatically to 20.7 MPa. A slight additional axial load was maintained to ensure that the sample connections were maintained for the injection ports.

After hydrostat was reached the axial load was slowly released to approximately 0.5 MPa axial stress. Once the extensile stress state was established, the injection pressure was increased to the pump maximum of 25.9 MPa in order to induce a fracture in the rock. Due to the limits of the injection pump the rock could not be fractured under these conditions, so the confining pressure was lowered from 20.7 MPa to 13.8 MPa, then to 6.9 MPa in order to generate the fracture.

4. RESULTS AND DISCUSSION

4.1. Granite Tests

The results from the proof of concept granite testing were very promising. Although the tests were not run under axisymmetric extension conditions, it showed that the jacketing process, frit, and proppant injection would worked. There was reasonable success in injecting proppant into the cracks, despite the cracks being oriented parallel to the bore hole. Fig.4 shows the axial load, confining pressure, injection pressure, and injection flow rate vs time for the second granite proof of concept test.

Fig. 4 shows the application of hydrostatic stress (red line). After hydrostatic stress was applied 3.3 MPa above confining stress was applied in the axial direction. This is followed by an increase in injection pressure. This increase in pressure failed to fracture the specimen, so the confining pressure was decreased to 6.9 MPa, with the axial differential stress remaining constant at 3.3 MPa over confining pressure. Injection pressure was then reapplied to the maximum that the pump could supply (25.9 MPa), and the specimen was successfully fractured, as evidenced by the precipitous drop in pressure. There was not a noticeable increase in flowrate when this occurred, because the pump flowrate was limited by the controller. After the dynamics of the fracture had settled, the injection pump settled into

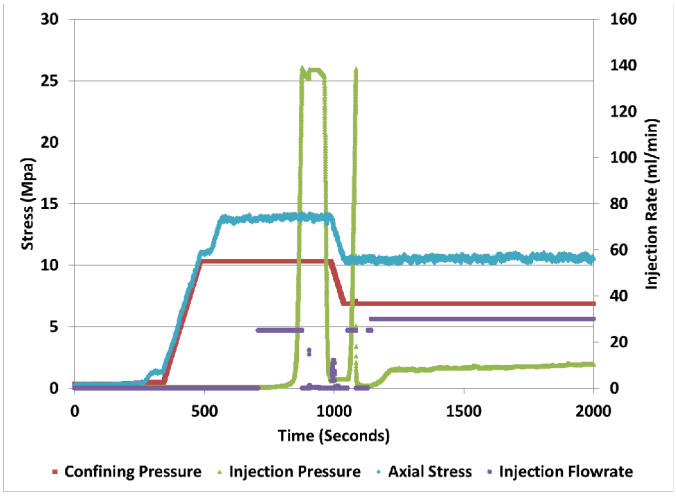

Fig. 4. Example injection and fracture curve for a granite specimen. The first peak in the injection pressure did not result in fracture, so the confining pressure and axial stress were lowered, then injection pressure was applied again, and the specimen fractured.

injection at a rate of 30 ml/min at a pressure of approximately 1.8 MPa. This pressure is not equal to the confining pressure because the fluid is allowed to escape the system through the frit. The fact that the fracture extends through the sample, combined with the drain, cause flow at pressures well below the confining pressure, because of surface discontinuities in the fracture surfaces. This is one main drawback of this fracturing process, as it does not allow for the measurement of the closure pressure.

Below in Fig. 5 the fracture can clearly be seen in µCT scans. The upper scan is shown normal to the borehole, and shows the fractures emanating out from the borehole as would be expected for this specimen under an axisymmetric compression state of stress. The lower scan, which was generated with a microfocus scan of one region of the specimen (right around the bottom of the borehole) shows that there is proppant in the bore and fracture. The grey particles in the bottom of the borehole and in the fracture around the borehole are proppant. The CT data is corroborated by visual observation of the fractures on the exterior of the specimen. It is difficult to capture in photographs but the proppant could be felt in and around the cracks on the exterior of the specimen post-test as seen in Fig 6.

4.2. Marcellus Shale

To date only one Marcellus shale specimen has been tested. That specimen was not injected with proppant as the primary goal of the first shale test was to ensure that the fracture could be generated in the proper orientation with the strong bedding effects present in the shale. This was of great concern because the specimen was cored parallel to bedding. This means that an especially weak bedding plane could have caused failure to occur parallel to the borehole, or it could have caused a fracture that

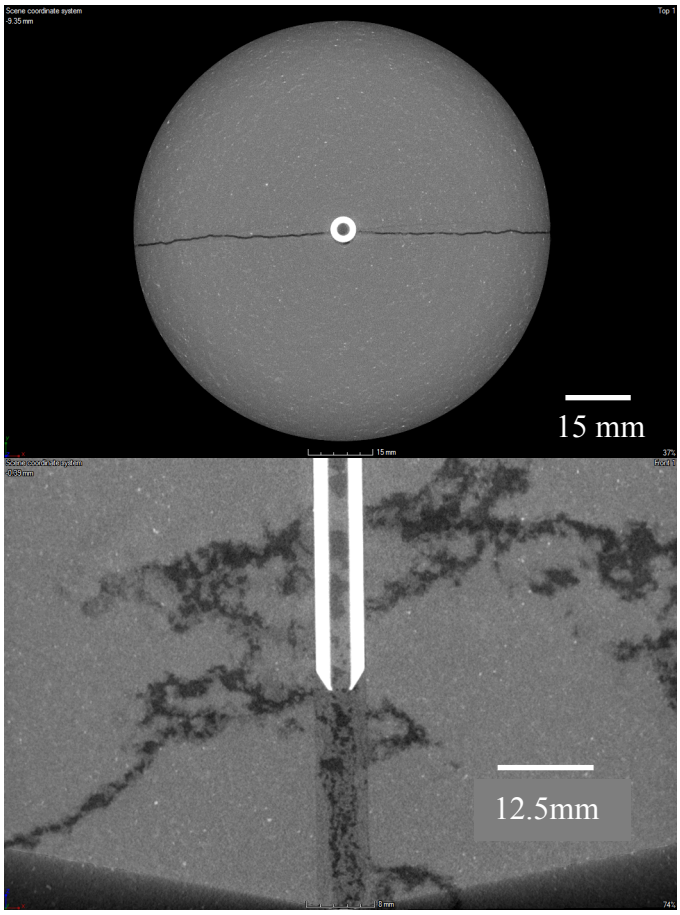

Fig. 5. µCT scans of a granite specimen. On top is a view looking down the bore axis, below a close up of the bottom of the borehole, where proppant can be seen distributed within the fracture.

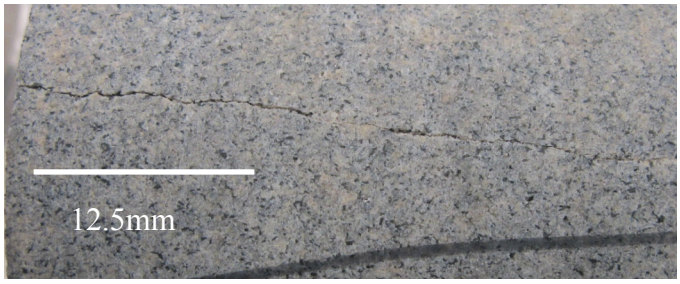

Fig. 6. Exterior of a granite specimen, showing the hydraulic fracture on the specimen surface.

had multiple orientations, i.e. started to fracture perpendicular to the core direction then followed a weak bedding plane.

It was also possible that the fracture would interact with natural fractures in the core and follow a different path. This was not desired, because the purpose of the test was to show that fracturing perpendicular to bedding is possible under these conditions in the laboratory, and interaction with natural fractures would have obscured that result. From the CT scan in fig. 7 it is apparent that the fracture formed in the desired direction, normal to the core direction, and bedding had little to no effect on the fracture. This image is from the middle of the

specimen, while no proppant was injected in this specimen it is apparent that there is sufficient space for proppant flow, and it shows that there is little interaction with pre-existing features in the core. The healed natural fractures, visible in the CT scan and on the surface of the specimen, fig. 8, appeared to have no effect on the hydraulic fracture.

It is clear from fig 8 that the preexisting natural fractures can conduct fluid, as evidenced by the wet fractures. However, the CT scan shows little to no opening of the preexisting fractures as seen in fig 7, implying that they are not affecting the local stress conditions. It is likely the reason for this is because the directionality of the fracture, and the stress conditions it was formed under were not favorable for opening preexisting fractures, or the preexisting fracture strength was high enough to prevent it from opening (Zhou et al. 2008). This suggests, for Marcellus, that preexisting fractures conduct fluid, but do not always open enough to conduct proppant. It is also possible that there is a scaling effect that is lost in the scale down for laboratory testing.

Fig. 9 shows the applied loads and flow rates for the Marcellus shale specimen. The confining pressure was

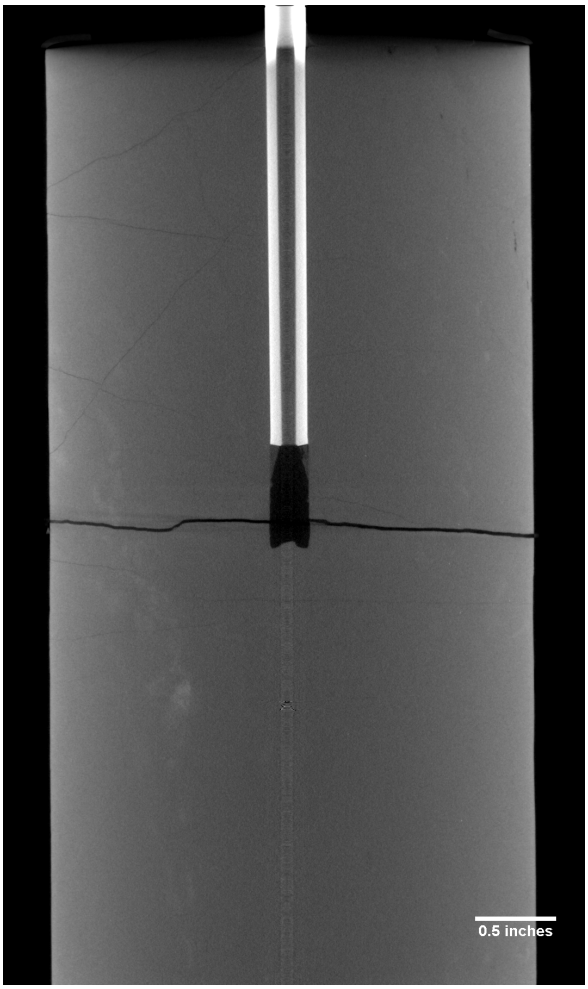

Fig. 7. CT scan of a fractured shale specimen.

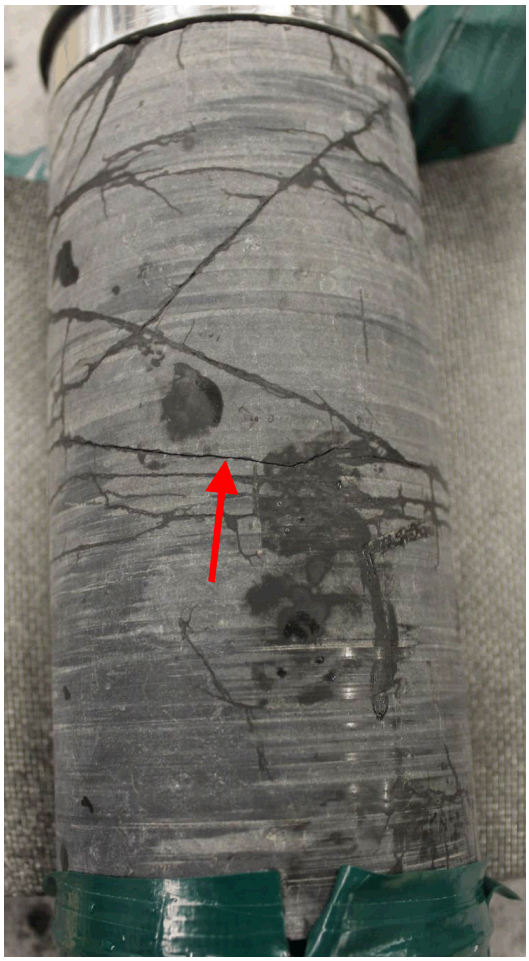

Fig. 8. Shale specimen post-test, the hydraulic fracture is clearly visible in the center of the specimen, marked by a red arrow, and the pre-existing natural fractures are possible conduits for water.

first increased to 20.7 MPa (red line), after which the axial stress was decreased to 0.5 MPa. Once this point was reached the injection pressure was increased to 25.9 MPa, which was insufficient to cause failure. Therefore the confining pressure was lowered to attempt to induce failure. This was done in two steps, first to 13.8 then to 6.9 MPa while the injection pressure was held constant. Fracturing can be seen as a number of small pressure drops in the injection pressure curve, followed by a precipitous drop in the injection pressure. It is known that this is not representative of the in situ conditions, lowering the confining pressure, but due to the strength of the rock and the limitations of the injection pump it was necessary. Fundamentally there is no difference between lowering the confining pressure and simply running the test at a lower initial confining pressure.

The pressure is increased back to the maximum pump pressure over a period of about 10 minutes. During this time the flow was allowed to increase to investigate the permeability of the fracture. It should be noted that as the injection pressure increases, so does the axial load, showing the transmission of the pressure from the crack to the load frame actuator. The pressures used in this test

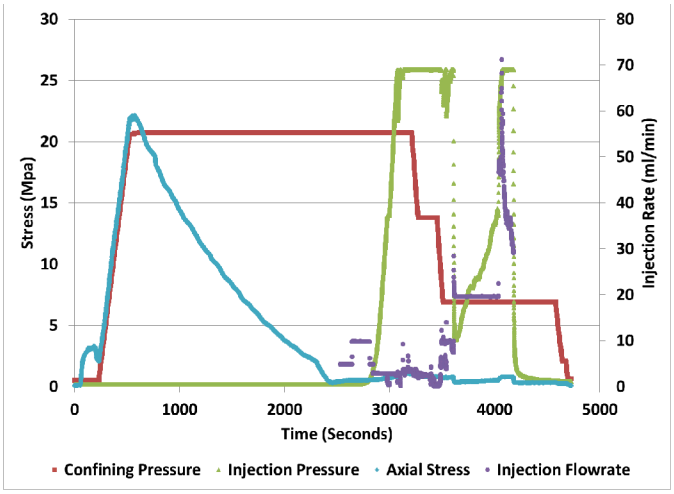

Fig. 9. Example injection and fracture curve for a Marcellus shale specimen.

are an artifact of the limits of the injection pump, and are not representative of the conditions in the earth. However, the only limitation on the system is the maximum pressure of the injection pump; subsequent tests will be run with a higher pressure pump so that in situ conditions can be achieved. The fracture orientation is the important result in this test. The same fracture orientation at higher pressures is a simple extension of this test.

5. CONCLUSIONS

This work shows that the disk on a string fracture pattern can be replicated in the laboratory under a representative in situ stress state. The stress magnitude was lower than in situ conditions. However, the low magnitude was due to system limitations, not limitations of the physics of fracture. This suggests that investigation of downhole phenomena in the laboratory can be performed with fewer simplifying assumptions.

This work also supports the findings of Zhou et al. (2008) who found that interaction of a hydraulic fracture with a natural fracture depended heavily on the stress state, inclination of the natural fracture with respect to the hydraulic fracture, and the strength of the natural fracture.

6. ACKNOWLEDGEMENTS

Sandia National Laboratories is a multi-program laboratory managed and operated by Sandia Corporation, a wholly owned subsidiary of Lockheed Martin Corporation, for the U.S. Department of Energy's National Nuclear Security Administration under contract DE-AC04-94AL85000. SAND2016-XXXX

REFERENCES

1. Alramahi, B., M.I. Sundberg. 2012. Proppant Embedment and Conductivity of Hydraulic Fractures in Shales. Presented at: *46th US Rock Mechanics/Geomechanics Symposium, Chicago, IL, USA, 24-27 June.*

2. ASTM D4543, 1995. Standard Practice for Preparing Rock Core Specimens and Determining Dimensional and Shape Tolerances, *American Society for Testing and Materials.*

3. Brown, R. L., B. Meckfessel. 2010. Improving Marcellus Shale Performance Using PDC Bits With Optimized Torque Management Technology, Cutting Structure Aggressiveness And Unique Roller Cone Steel Tooth Cutting Structures. Presented at: *Society of Petroleum Engineers Eastern Regional Meeting, Morgantown, WV, USA, 13-15 October.*

4. Fredd, C.N., S.B. McConnell, C.L. Boney, K.W. England. 2000. Experimental Study of Hydraulic Fracture Conductivity Demonstrates the Benefits of Using Proppants. Presented at: *SPE Rocky Mountain Regional/Low Permeability Reservoirs Symposium, Denver, CO, USA, 12-15 March.*

5. Haimson, B., C. Fairhurst, 1969, Hydraulic fracturing in porous-permeable materials, *J. Petrol. Technol.* 21(07): 811–817

6. Heap, M.J., D.R. Faulkner, 2008. Quantifying the evolution of static elastic properties as crystalline rock approaches failure, *International Journal of Rock Mechanics and Mining Sciences*, 45(4):564-573

7. Kehle, R.O. 1964, The determination of tectonic stresses through analysis of hydraulic well fracturing, *J. Geophys. Res.*, 69: 259–273.

8. Krech, W.W., F.A. Henderson and K.E. Hjelmstad, (1974), A Standard Rock Suite for Rapid Excavation Research, *U.S. Bureau of Mines*, RI-7865

9. Lane, N., K.E. Thompson, 2010. Image-Based Pore-Scale Modeling using the Finite Element Method. In: *Advances in Computed Tomography for Geomaterials: GeoX 2010*. Eds. K.A. Alshibli and A.H. Reed.

10. Morris, J., and N. Chugunov. 2014. Comparison of Heterogeneously-Propped Hydraulic Fractures for Vertical and Lateral Wells. Presented at: *AGU Fall Meeting, 2014. San Francisco, CA, USA, 15-19 December.*

11. Pegler, A.V. 1967. A Laboratory Study of the Fracturing of Rocks by Hydraulic Pressure. In *Proceedings of the 9th US Rock Mechanics Symposium*, Golden, CO, USA, 17-19 April 1967.

12. Sitchler, J. C., B.V. Cherian, M.L. Panjaitan, C.M. Nichols, & J.K. Krishnamurthy. 2013. Asset Development Drivers in the Bakken and Three Forks. Presented at: *Society of Petroleum Engineers Fracturing Technology Conference, The Woodlands, TX, USA, 4-6 February.*

13. Wang, G., T.R. Carr, 2012. Methodology of organic-rich shale lithofacies identification and prediction: A

case study from Marcellus Shale in the Appalachian basin, *Computers & Geosciences*, 49: 151-163.

14. Wen, Q., S. Zhang, L. Wang, Y. Liu, X. Li. 2006. The effect of proppant embedment upon the long-term conductivity of fractures. *J. Pet. Sci. and Eng.* 55: 221-227.

15. Zhou, J., M. Chen, Y. Jin, G. Zhang, Analysis of fracture propagation behavior and fracture geometry using a tri-axial fracturing system in naturally fractured reservoirs, *International Journal of Rock Mechanics and Mining Sciences*, Volume 45, Issue 7, October 2008, Pages 1143-1152

16. Zoback, M.D., F. Rummel, R. Jung, C.B. Raleigh, 1977. Laboratory hydraulic fracturing experiments in intact and pre-fractured rock, *International Journal of Rock Mechanics and Mining Sciences & Geomechanics Abstracts*, 14(2): 49-58